Journal of Colloid and Interface Science 493 (2017) 17–23

Contents lists available at ScienceDirect

Journal of Colloid and Interface Science

journal homepage: www.elsevier.com/locate/jcis

Regular Article

Adsorption of phosphate from aqueous solution using iron-zirconium modified activated carbon nanofiber: Performance and mechanism

Weiping Xiong [a,b], Jing Tong [a,b], Zhaohui Yang [a,b,*], Guangming Zeng [a,b,*], Yaoyu Zhou [c], Dongbo Wang [a,b], Peipei Song [a,b], Rui Xu [a,b], Chen Zhang [a,b], Min Cheng [a,b]

[a] College of Environmental Science and Engineering, Hunan University, Changsha 410082, China
[b] Key Laboratory of Environmental Biology and Pollution Control, Ministry of Education, Hunan University, Changsha 410082, China
[c] College of Resources and Environment, Hunan Agricultural University, Changsha 410128, China

GRAPHICAL ABSTRACT

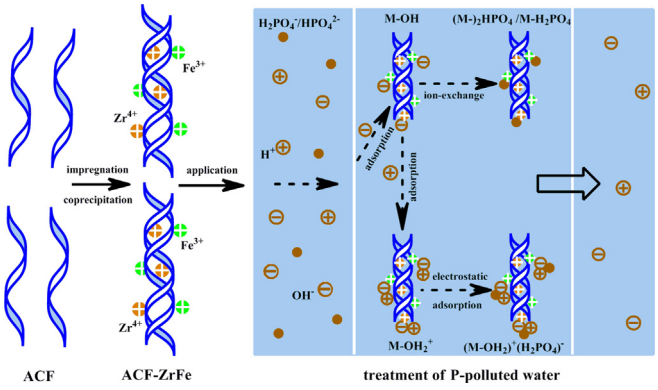

ARTICLE INFO

Article history:
Received 13 December 2016
Revised 5 January 2017
Accepted 6 January 2017
Available online 7 January 2017

Keywords:
Phosphate
Adsorption
Iron
Zirconium
Activated carbon nanofiber

ABSTRACT

Phosphate (P) removal is significant for the prevention of eutrophication in natural waters. In this paper, a novel adsorbent for the removal of P from aqueous solution was synthesized by loading zirconium oxide and iron oxide onto activated carbon nanofiber (ACF-ZrFe) simultaneously. The adsorbent was characterized by scanning electron microscopy (SEM), Fourier transform infrared (FT-IR) spectroscopy and X-ray photoelectron spectroscopy (XPS). The results showed that P adsorption was highly pH dependent and the optimum pH was found to be 4.0. The isotherm of adsorption could be well described by the Langmuir model and the maximum P adsorption capacity was estimated to be 26.3 mg P/g at 25 °C. The kinetic data were well fitted to the pseudo-second-order equation, indicating that chemical sorption was the rate-limiting step. Moreover, co-existing ions including sulfate (SO_4^{2-}), chloride (Cl^-), nitrate (NO_3^-) and fluoride (F^-) exhibited a distinct effect on P adsorption with the order of $F^- > NO_3^- > Cl^- > SO_4^{2-}$. Further investigations by FT-IR spectroscopy and pH variations associated with the adsorption process revealed that ligands exchange and electrostatic interactions were the dominant mechanisms for P adsorption. The findings reported in this work highlight the potential of using ACF-ZrFe as an effective adsorbent for the removal of P in natural waters.

* Corresponding authors at: College of Environmental Science and Engineering, Hunan University, Changsha 410082, China.
E-mail addresses: yzh@hnu.edu.cn (Z. Yang), zgming@hnu.edu.cn (G. Zeng).

http://dx.doi.org/10.1016/j.jcis.2017.01.024
0021-9797/

1. Introduction

Phosphate (P), an indispensable macronutrient widely found in aquatic environments, is highly required for the growth of living organisms and the normal functioning of ecosystems. However, about 1.3 Mt of P in every year from all over the world discharged into aquatic systems will lead to over-fertilization and cause eutrophication and ecosystem degradation [1–4]. Therefore, it is necessary to take highly effective, reliable, and economical methods to remove P from wastewater prior to its discharge.

Stringent regulations have been implemented by many countries with respect to the presence of P in water. These strict regulations have triggered a variety of P removal technologies, including chemical precipitation which relies on ferric or aluminum salts [1,5], adsorption methods [6–10], biological treatments [11–13], and ion exchange [14]. Among these available treatment methods, adsorption is considered to be an effective approach due to its easily–handle operation, low cost and eco-friendly characters [15–18]. Various adsorbents such as fly ash [19], aluminum hydroxide [20], iron-based compounds [21–24] and Ca-based sorbents [25] have been tested for P adsorption. However, the direct addition of adsorbents in water treatment system may cause fast loss of adsorbents and reduce their reusability as a result of their tiny powder size, which usually restrict the application of adsorbents [26]. To further improve the recyclability and adsorption capacity, it is of particular significance to develop more novel phosphate-specific adsorbents. In recent investigations, zirconium-based materials have been paid more attention in controlling P pollution due to their high binding affinity towards P, non-toxicity and acceptable cost. Awual et al. [27] reported fibrous loaded with zirconium for P removal from water. Su et al. [28] synthesized amorphous zirconium oxide nanoparticles via a simple and low-cost hydrothermal process and the new adsorbent exhibited remarkable P adsorption capacity under various conditions. In addition, iron-based materials have been reported as showing good P removal efficiency and possessing advantageous characteristics in terms of cost, chemical stability and environmental consequence [29]. In order to inherit the advantages of these two kinds of adsorbents, a composite sorbent containing zirconium and iron oxides was developed and exhibited promising performance for P adsorption [15].

Activated carbon nanofiber (ACF), which is a highly microporous carbon material and shows favorable adsorption performances due to its nano-structure, abundant micrometer porosity, high specific surface area and uniform micropore size distributions [30,31], is believed to have potential applications in adsorption. The particular characteristics of ACF mentioned above are due to the versatility of being loaded with metal oxide. For instances, metal oxides such as titanic oxide [31], manganese oxide [32], iron oxides [33] and Lanthanum iron oxides [34] have been successfully introduced to the surface of ACF. Manganese-modified ACF was found to have a high efficiency of arsenic removal by providing abundant amounts of binding sites on the obtained Mn-ACF adsorbent surface [32]. The adsorption capacity for P of Lanthanum oxide doped ACF [34] was enhanced, which was principally attributed to the formation of new coordination sites from the hydroxyl groups on lanthanum oxide. Nevertheless, no report is available on the study of the phosphate adsorption by Fe—Zr modified ACF which may have promising adsorption capacity, as the functional groups may be formed in ACF after the modification.

In this study, a new adsorbent for the removal of P from aqueous solution was prepared by loading zirconium and iron particles on the surface of ACF (ACF-ZrFe) simultaneously. The main objectives of this study are to: (i) characterize the synthesized adsorbent by scanning electron microscopy (SEM), X-ray photoelectron spectroscopy (XPS) and Fourier transform infrared spectroscopy (FT-IR); (ii) systematically evaluate the influences of various experimental parameters, such as initial P concentration, pH values, reaction time and co-existing substances on adsorption performance; (iii) reveal the mechanisms of P adsorption onto ACF-ZrFe.

2. Experimental procedures

2.1. Materials

All reagents such as zirconium oxychloride octahydrate, ferric nitrate, potassium phosphate monobasic and ammonium hydroxide were of analytical grade and purchased from Sinopharm Chemical Reagent Co., Ltd, China. ACF was procured from Nantong Senyou Carbon Fiber Co., Ltd., Nantong, China. This ACF has aspecific surface area of 1300–1400 m^2/g, with thickness of 1–5 mm. Stock solution of P was prepared using anhydrous KH_2PO_4 and pH was pre-adjusted by HCl or NaOH solutions. All water samples containing P were filtrated through 0.45 μm membrane filters and then quantitatively determined by the molybdenum blue method [35] on a SHIMAD UV-2401PC UV/Vis spectrometer with the detection wavelength of 700 nm. All solutions were prepared using deionized water.

2.2. Synthesis of adsorbent

ACF was first cut into desired size pieces (0.5 cm × 0.5 cm), which was then fully washed four times with deionized water and kept in boiling water for 30 min to remove impurities and soluble salts. The treated ACF was dried at 100 ± 5 °C for 4 h. The zirconium-iron-modified ACF (ACF-ZrFe) was prepared by a one-step synthesis method as follows. 0.5 g of ACF was subsequently immersed into zirconium oxychloride octahydrate and ferric nitrate mixed solution. After 24 h of reaction, the obtained zirconium-iron-modified ACF medium was combined with a 1 M NaOH solution for 2 h to precipitate the mixed ions. The product was filtered and washed repeatedly with distilled water to lower the pH below 8.0. After drying at 105 °C for 24 h, the zirconium-iron-modified ACF (ACF-ZrFe) adsorbent was obtained.

2.3. Characterization

The morphology of the sample was characterized using a scanning electron microscope (SEM, JSM-6400F). The FT-IR spectrum of ACF-ZrFe adsorbent before and after phosphate adsorption were measured by a Nicolet 6700 FT-IR spectrometer. XPS analysis was conducted using an ESCALAB 250Xi X-ray photoelectron spectroscopy equipped with a monochromatized Al Ka X-ray source, all the binding energies were referenced to the C 1s peak at 284.8 eV of the surface adventitious carbon.

2.4. Batch sorption experiments

All the phosphate adsorption tests were carried out at room temperature in 250 mL conical flasks. Phosphate solution of 100 mL was used for each experiment with varying dose of ACF-ZrFe. Batch adsorption experiments were carried out at different initial pH values ranging from 2.0 to 12.0. The solution pH was adjusted by adding HCl (0.10 M) or NaOH (0.10 M) solutions. Considering that abundant salt additives are often present in natural waters, it is important to examine the performance of ACF-ZrFe under high ionic strength, thus, Na_2SO_4, NaCl, NaF or $NaNO_3$ solutions were added as sources of the competing anions when necessary. The mixture was shaken at a thermostatic shaker with certain

speed to ensure fully contact between ACF-ZrFe and phosphate in water. After adsorption experiment, the mixture was filtered through a 0.45 μm membrane syringe filter and residual P was analyzed for the adsorption efficiency.

To determine the reaction time at adsorption equilibrium, kinetic experiments of phosphate adsorption on ACF-ZrFe were conducted as follows: 300 mL phosphate solution (initial concentrations: 10, 20 and 30 mg/L, respectively) containing 0.3 g adsorbent in flasks were shaken at 150 rpm in a thermostatic shaker at room temperature. A 2 mL of solution was withdrawn and filtered at given intervals for the analysis of phosphate concentrations. As for the equilibrium experiments, the same experimental procedure was performed as aforementioned procedures by varying the initial concentration of phosphate (5–60 mg/L).

2.5. Desorption and regeneration studies

The feasibility of regenerating ACF-ZrFe for repeated use was investigated by using concentrations of different NaOH (0, 0.001, 0.01, 0.1 or 0.5 M). Specifically, after accomplishment of the adsorption experiments, the P-loaded adsorbent was magnetically separated and subsequently added into 50 mL NaOH solution and the desorption time was 12 h. After washing thoroughly with ultrapure water to neutrality, the regenerated adsorbent was recycled and reused.

2.6. Goodness-of-Fit Measure (GoFM)

The model parameters for Freundlich, Langmuir and Elovichi-sotherm have been determined by minimizing the difference between the experimental and modeled Q_e values (through the average relative error (ARE)) using the iterative method [36].

The average relative error (ARE)

$$ARE = \sum_{i=1}^{n} \left| \frac{Q_{e,\exp} - Q_{e,calc}}{Q_{e,\exp}} \right|_i \quad (1)$$

where "exp" and "calc" show the experimental and calculated values, respectively.

Besides, a minimization procedure has been adopted to solve kinetic equations by minimizing the sum of error squared (SSE) between the predicted values and the experimental data using the solver add-in function of the Microsoft Excel [37].

$$SSE = \sqrt{\frac{\sum \left(Q_{\exp} - Q_{\text{calc}}\right)^2}{N}} \quad (2)$$

where the subscripts "exp" and "calc" are the experimental and calculated values of Q, respectively and N is the number of measurements.

3. Results and discussion

3.1. SEM analysis for ACF-ZrFe

The SEM images of ACF, ACF-ZrFe and the sample after P adsorption (named as ACF-ZrFeP) were shown in Fig. 1. The SEM micrograph revealed that the ACF surface was smooth and it possessed a superior specific area. Compared to Fig. 1a, Fig. 1b presented a rough surface due to the loading of Zr—Fe complex hydroxide particles with an irregular shape on ACF. Moreover, it can be seen from Fig. 1b and c that a vast majority of Zr—Fe mixed ions are still firmly immobilized on the ACF surface after adsorption process, demonstrating that ACF-ZrFe is an environment-friendly material.

3.2. Kinetics studies on phosphate adsorption by ACF-ZrFe

Phosphate removal by adsorbent as a function of contact time with different initial concentration (10, 20 and 30 mg/L) is shown in Fig. 2. It was noteworthy that the three curves exhibit the same trend. The amount of adsorbed P increased rapidly in the early stage of the P adsorption reaction, probably due to the availability of abundant active sites on the ACF-ZrFe surface. However, the adsorption rate became slower as a result of the decrease of active sites with adsorption time. Similar results were obtained by Su et al. [28].

To investigate the mechanism of adsorption, kinetic models have been exploited to analyse the experimental data. In addition, information on the kinetics of P uptake is required to select the optimum condition for scaling up the P removal processes [38,39]. Several kinetic models such as pseudo-first-order, pseudo-second-order and elovich model have been applied to

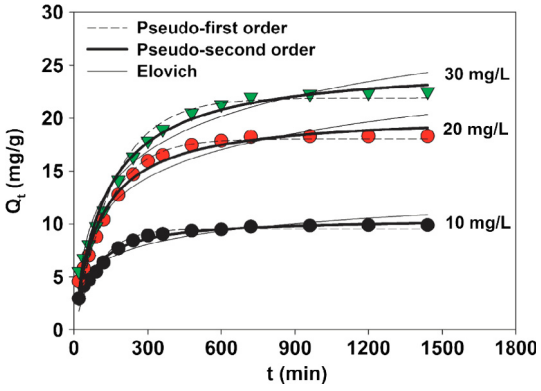

Fig. 2. Phosphate adsorption kinetics. Initial concentration of phosphate, 10, 20, 30 mg/L, respectively, containing 0.3 g adsorbent in flasks were shaken vigorously in a thermostatic shaker at room temperature and pH 6.80 ± 0.20.

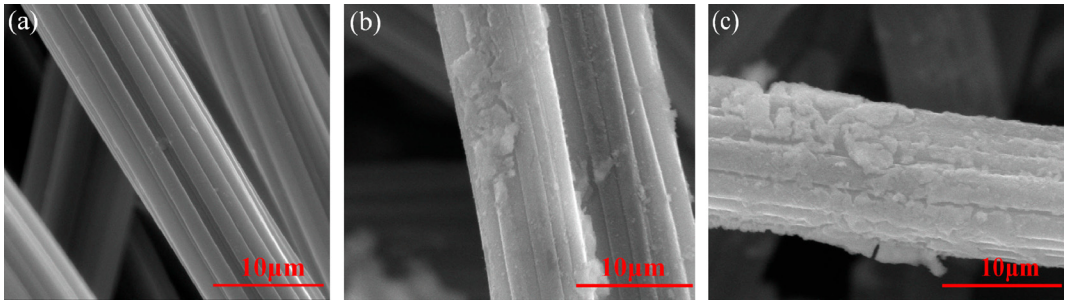

Fig. 1. SEM of (a) ACF with aspecific surface area of 1300–1400 m^2/g and thickness of 1–5 mm, (b) ACF-ZrFe (ACF 0.5 g; S/L ratio 5.0 g L^{-1}; pH 10.0) and (c) ACF-ZrFeP (n(Zr):n(Fe) = 7:3; pH 4.0; 25 °C).

investigate the adsorption mechanism [37,40,41]. The equations of the three kinetic models are expressed in Text S-1, supporting information.

The parameter values obtained from the application of kinetic models were used to predict the variation of adsorbed P with time. The resulting curves and kinetic parameters are presented in Fig. 2 and Table 1, respectively. The correlation coefficient (R^2) suggested that the pseudo-second-order model (R^2 = 0.9834–0.9850) was better fitted with the experimental data compared to the pseudo-first-order model (R^2 = 0.9554–0.9793) and elovich model (R^2 = 0.9554–0.9625). Meanwhile, the adsorption capacity calculated from pseudo-second-order equation was more consistent with the experimental Q_e value since the SSE of the pseudo-second-order model was less than that of all other models. Similar kinetic study results on various phosphate adsorbents had been reported by Su et al. [28], Rodrigues [42] and Tang et al. [43]. The pseudo-second-order rate model demonstrates chemisorptions occurred between phosphate and ACF-ZrFe nanoparticles involving exchange of electrons or valency forces through sharing between sorbent and sorbate, in fact, there placement of —OH by phosphate, which will be discussed in detail in the following sections in the adsorption mechanism study.

3.3. Equilibrium adsorption isotherm study on phosphate adsorption by ACF-ZrFe

The adsorption isotherm indicates how the adsorbate molecules are distributed between the liquid phase and the solid phase at given pH values and temperatures, which was obtained by varying the initial concentrations of P (5–60 mg/L) at room temperature. The equilibrium adsorption data for the adsorption of P by ACF-ZrFe were analyzed by the Langmuir, Freundlich and Temkin isotherm equations [44,45].

The Langmuir adsorption model is an ideal adsorption model which is appropriate for the monolayer adsorption onto the adsorbent surface. The Langmuir model assumes that adsorbent is structurally homogenous and the adsorption process ends up in monolayer coverage with uniform adsorption energies [46]. The Langmuir equation can be expressed by Eqs. (2) and (3), in Text S-1, supporting information. The Freundlich adsorption isotherm has been interpreted as sorption to heterogeneous surfaces or surface supporting sites with different affinities and can be derived assuming a logarithmic decrease in the enthalpy of sorption with the increase in the fraction of occupied sites. The Freundlich isotherm is expressed in Text S-1, supporting information. The Temkin isotherm contains a factor that the interactions between the adsorbent and the adsorbed particles [47]. The equations are expressed in Text S-1, Supporting information.

Table 1
Kinetic parameters of P adsorption on ACF-ZrFe.

	10[a]	20[a]	30[a]
$Q_{e,exp}$	9.88	18.30	22.5
Pseudo-first order			
$Q_{e,calc}$	10.56	20.39	25.24
k_1	0.0104	0.0075	0.0063
SSE	0.1756	0.5396	0.7075
R^2	0.9554	0.9793	0.9666
Pseudo-second order			
$Q_{e,calc}$	9.54	18.05	21.92
k_2	1.53×10^{-3}	0.54×10^{-3}	0.36×10^{-3}
SSE	0.0878	0.0645	0.1498
R^2	0.9850	0.9834	0.9834
Elovich			
$Q_{e,calc}$	10.87	20.35	24.31
a	0.3570	0.5574	0.5547
b	0.8483	0.2630	0.2109
t_0	3.3019	6.8210	8.5480
SSE	0.2556	0.5293	0.4673
R^2	0.9397	0.9431	0.9625

[a] C0 (initial concentration) (mg/L).

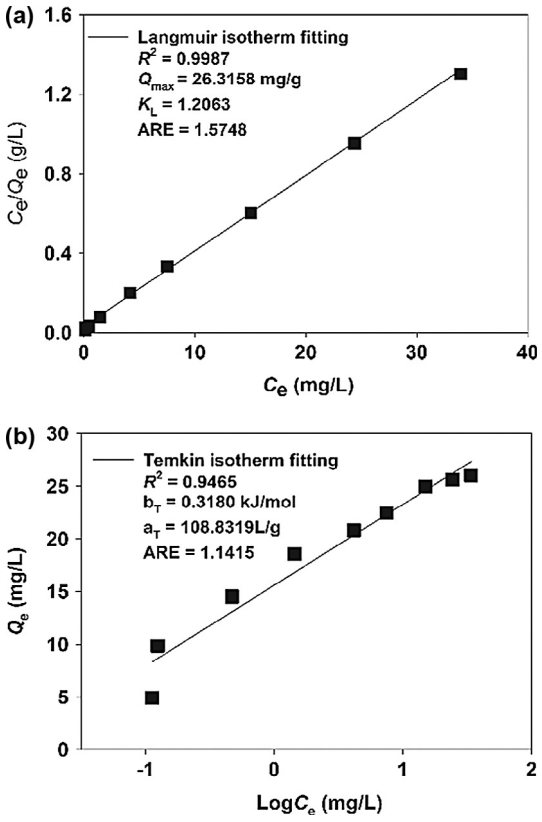

Fig. 3. Isotherms of phosphate on ACF-ZrFe, (a) linear Langmuir adsorption isotherms and (b) Temkin adsorption isotherms.

The adsorption isotherms and the isotherm constants were shown in Fig. 3 and Fig. S-1, respectively. It was evident that compared with the Freundlich model, the Langmuir model and Temkin model fitted the experiment data better in view of its higher correlation coefficient (R^2) and lower values of the average relative error (ARE). For Langmuir model, it suggested that the homogeneous adsorption of PNP occurred on the adsorbent. As for Temkin model, typical physisorption processes are reported to have adsorption energies less than −40 kJ mol^{-1}, while bonding energy range for ion-exchange mechanism is reported to be in the range of 8–16 kJ mol^{-1}. Values of b_T obtained in the present study was 0.3180 kJ mol^{-1} indicates that the adsorption process seems to involve chemisorption and physisorption. In addition, the sorption capacities of P on ACF-ZrFe were compared with other adsorbents previously reported in the literature and the results was presented in Table S-1. It was noticed that ACF-ZrFe had a little higher removal efficiency for P in our experiments.

3.4. FT-IR analysis

The FTIR spectrum of ACF-ZrFe before and after phosphate adsorption were shown in Fig. 4. By comparing the FT-IR spectra of ACF with ACF-ZrFe, the new peak at 1383 cm^{-1} was attributed to the vibration modes of NO_3^- (nitrate) from the raw materials of $Fe(NO_3)_3$ [48] and the intensive band in 1338 cm^{-1} region indicated the presence of surface hydroxyl on the metal oxide surface (Zr—OH) [49]. Furthermore, the peak at 512 cm^{-1} was attributed to

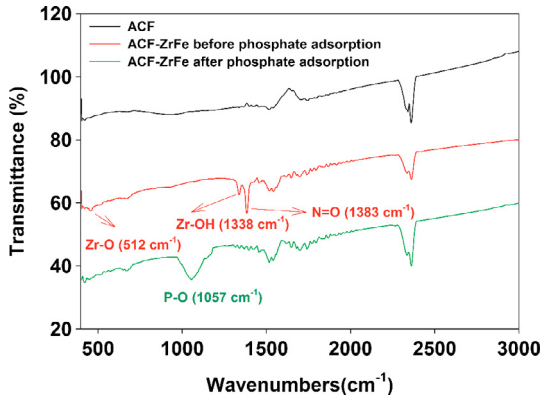

Fig. 4. Presents the FT-IR spectra of (a) ACF with aspecific surface area of 1300–1400 m^2/g and thickness of 1–5 mm, (b) ACF-ZrFe (ACF 0.5 g; S/L ratio 5.0 g L^{-1}; pH 10.0) and (c) ACF-ZrFeP (n(Zr):n(Fe) = 7:3; pH 4.0; 25 °C).

the vibrations of Zr—O functional group [50]. This indicates that the Zr and Fe are indeed loaded onto the surface of the ACF, which is also manifested with the presence of Zr and Fe particles from the SEM image of ACF-ZrFe. It could be seen that after adsorption, the FT-IR spectrum of ACF-ZrFe is changed obviously. The Zr—OH deformation peak disappeared, while the peaks of NO_3^- dramatically weakened. These observations indicated that the replacement of —OH and NO_3^- occurred during the P adsorption. Additionally, a new peak appeared at 1057 cm^{-1}, which was broad and strong. This new peak could be assigned to the asymmetry vibration of P—O on ACF-ZrP, indicating that the surface hydroxyl groups were replaced by the adsorbed P.

3.5. XPS analysis

The surface O 1s spectrum of ACF-ZrFe before and after phosphate adsorption at natural pH (6.80 ± 0.20) were analyzed by high-resolution XPS scan and were presented in Fig. 5. As seen in Fig. 5a, the O 1s spectra was divided into two peaks at 529.7 eV (O^{2-}) and 531.2 eV (—OH), respectively [28], suggesting that both O^{2-} and —OH coexist on the ACF-ZrFe and the content of —OH (79.58%) is larger than that of O^{2-} (20.42%). However, as seen in Fig. 5b, it can be seen that the —OH percentage dropped from 79.58% to 66.30% after the phosphate sorption, while the area ratio of O^{2-} increased from 20.42% to 33.7%. The decrease of hydroxyl group amount could be attributed to the replacement of —OH by phosphate during the adsorption process. Thus, the surface hydroxyl group plays a key role in the phosphate adsorption, which is in accordance with the results of FT-IR studies.

3.6. Effect of pH on phosphate adsorption by ACF-ZrFe

The effect of pH on phosphate adsorption by ACF-ZrFe was shown in Fig. 6. Batch adsorption experiments were carried out at different initial pH values ranging from 2.0 to 12.0. It can be concluded from Fig. 6 that P adsorption reaction is evidently pH dependent. Under the acidic pH conditions, P removal increased from pH 2.0 to pH 4.0 and the maximum value was achieved at pH 4.0. Further increase of pH decreased P adsorption. Similar solution pH effect had also been observed in previous reports for various adsorbents [51].

It is well known that P can exist in the form of H_3PO_4, $H_2PO_4^-$, HPO_4^{2-} and PO_4^{3-} at different solution pH values, indicating that P dissociation equilibrial in liquid are pH-related and they can be shown as the following equations [45]:

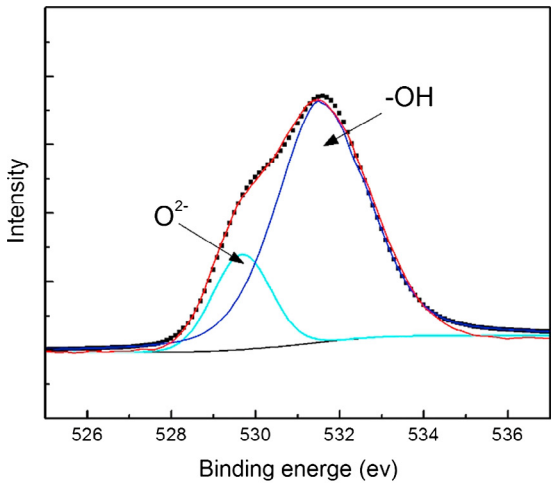

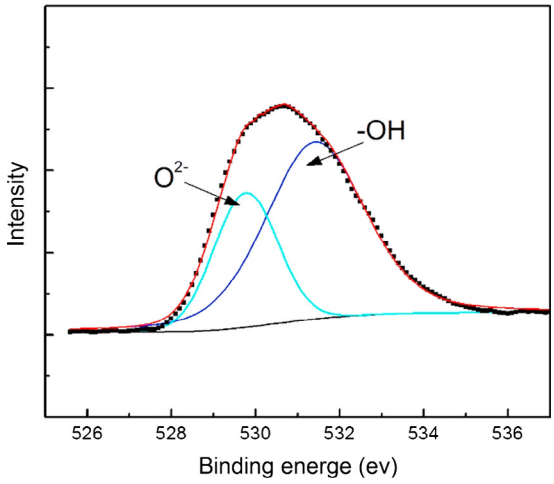

Fig. 5. The surface O 1s spectra of ACF-ZrFe (a) before and (b) after phosphate adsorption with initial phosphate concentration at 10 mg/L, adsorbent dose at 0.5 g/L, and pH 6.80 ± 0.20.

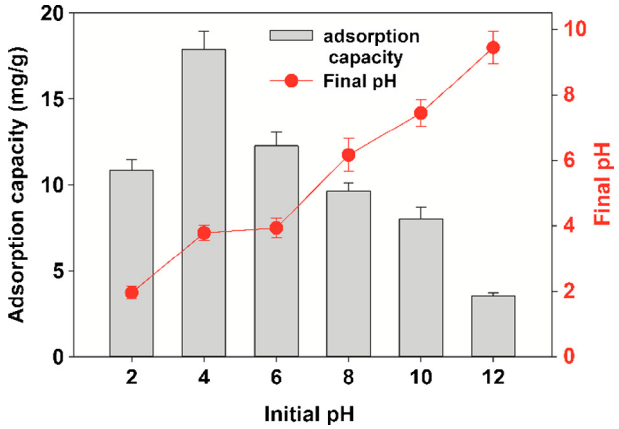

Fig. 6. Effect of initial pH on phosphate adsorption on ACF-ZrFe and final pH variation of solution. All batch experiments were performed in duplicates. Error bars represent the standard deviation of triplicate samples.

$$H_3PO_4 \overset{k_1}{\leftrightarrow} H_2PO_4^{2-} \overset{k_2}{\leftrightarrow} HPO_4^{2-} \overset{k_3}{\leftrightarrow} PO_4^{3-} \quad (3)$$

where $pK_1 = 2.15$, $pK_2 = 7.20$ and $pK_3 = 12.33$, respectively.

It is obvious that the solution pH will determine the major species of phosphate and affect the strength of electrostatic

attraction. When pH is lower than 2.15, the dominant P forms in the solution are the neutral H_3PO_4 which is weakly attached to the sites of ACF-ZrFe because of no electrostatic forces and ion exchange in the removal process. With the increase of solution pH, the dominant species transformed into $H_2PO_4^-$ and HPO_4^{2-} and the surface of ACF-ZrFe was positively charged via protonation. Hence, $H_2PO_4^-$ and HPO_4^{2-} were adsorbed on ACF-ZrFe by electrostatic forces and the ion exchange. The coulombic attraction between the negative phosphate anions and the positive protonated ACF-ZrFe surface can be shown as:

$$M - OH + H^+ \leftrightarrow M - OH_2^+ \quad (4)$$

$$M - OH_2^+ + H_2PO_4^- \leftrightarrow (M - OH_2)^+(H_2PO_4)^- \quad (5)$$

The ion-exchange mechanism can be expressed as follows:

$$M - OH + H_2PO_4^- \leftrightarrow M - H_2PO_4 + OH^- \quad (6)$$

$$2M - OH + HPO_4^{2-} \leftrightarrow (M-)_2HPO_4 + 2OH^- \quad (7)$$

This ion-exchange mechanism was further confirmed by the FT-IR results which demonstrated that the hydroxyl groups of Zr—OH disappeared after phosphate adsorption process. However, as the concentration of OH^- increased at alkaline pH, the effect of electrostatic attraction between anions and adsorbent became negligible due to deprotonation of the adsorbent surface and the strong competition of hydroxide with phosphate. Simultaneously, the ligand exchange mechanism became impractical [52], eventually leading to a lowered phosphate removal.

In conclusion, the distribution of phosphate species changed with the pH variations, whereas different phosphate species behave distinct affinities toward the ACF-ZrFe, this process was controlled by the two interactions mentioned above, i.e., electrostatic attraction and ion exchange. With the increase of pH, the effects of electrostatic and ion exchange weakened. It can also be observed that the pH of the solution was lower than the initial pH value, which was due to the release of positively charged proton from the surface of ACF-ZrFe.

3.7. Effect of coexisting ions

Natural water normally contains many other anions, which may compete with P for the active adsorption sites. Therefore, it is necessary to investigate the potential influence of coexisting anions on the adsorption process of ACF-ZrFe towards phosphate. In this study, the effects of sulfate, chloride, nitrate and fluoride on P adsorption were examined and the results were summarized in Fig. S-2. As shown in Fig. S-2, the phosphate adsorption capacity was decreased when the concentration of competitive ions was 100 mg/L. The presence of coexisting anions had different effects on phosphate adsorption and the inhibition in P adsorption follows the following order: $F^- > NO_3^- > Cl^- > SO_4^{2-}$. Obviously, F^- among these anions caused the greatest decrease of P adsorption and the adsorption of P decreased from 16.82 mg/g to 8.51 mg/g. It is clear that ACF-ZrFe interacts with P mainly through the exchange between the P ions and the hydroxide ions at the Zr(IV) and Fe (III) site. Hence, the effect of these anions on P adsorption is due to their affinity towards the adsorbent material and competes effectively with the P adsorption.

3.8. Desorption of phosphate from ACF-ZrFe and their reuse

In this study, NaOH solutions of different concentrations were used to desorb the phosphate adsorbed on ACF-ZrFe and the results was presented in Fig. S-3. With the increase of the alkalinity of NaOH solution, the amount of desorbed phosphate increased. Without NaOH addition, only 5.18% of adsorbed phosphate was desorbed. When the NaOH concentration increased to 0.1 M, the desorption phosphate enhanced to 91.40%. However, further increase of NaOH to 0.5 M did not increase the desorption of phosphate significantly. The results indicated that 0.1 M NaOH could be used to desorb the phosphate adsorbed on ACF-ZrFe. Besides, the desorbed ACF-ZrFe was reused for the removal of phosphate, which indicated that ACF-ZrFe could keep 87% of its original phosphate removal capability after being desorbed by NaOH for two times. Therefore, the recovered ACF-ZrFe could be reutilized to remove phosphate from water and thus could reduce the operation cost significantly.

4. Conclusions

The novel sorbent ACF-ZrFe was successfully synthesized by loading zirconium oxide and iron oxide onto activated carbon nanofiber and employed to remove phosphate from aqueous solution. The maximum adsorption capacity for ACF-ZrFe was about 26.3 mg P/g with the pH of 4.0, which was higher than that of ACF-hydrated ferric oxide [33] and ACF-lanthanum and iron oxides [34]. The predominant mechanism for P adsorption on the ACF-ZrFe included electrostatic interaction and ion exchange. The effect sequence of coexisting anions competing with phosphate for adsorption sites was: $F^- > NO_3^- > Cl^- > SO_4^{2-}$. Moreover, ACF-ZrFe could be reused for the removal of phosphate. In conclusion, the ACF-ZrFe is an environment-friendly, reliable and efficient adsorbent, which is suitable for P removal from aqueous solution and potentially other pollutants from contaminated water or soils. The activated carbon nanofiber based nanocomposites has broad prospect of application in environmental science and engineering.

Acknowledgements

The study was financially supported by the National Natural Science Foundation of China (51521006, 51378190), the Program for Changjiang Scholars and Innovative Research Team in University (IRT-13R17) and the Fundamental Research Funds for the Central Universities.

Appendix A. Supplementary material

Supplementary data associated with this article can be found, in the online version, at http://dx.doi.org/10.1016/j.jcis.2017.01.024.

References

[1] P. Wilfert, P.S. Kumar, L. Korving, G.J. Witkamp, M.C. van Loosdrecht, The relevance of phosphorus and iron chemistry to the recovery of phosphorus from wastewater: a review, Environ. Sci. Technol. 49 (2015) 9400–9414.
[2] M. Cheng, G. Zeng, D. Huang, C. Lai, P. Xu, C. Zhang, Y. Liu, Hydroxyl radicals based advanced oxidation processes (AOPs) for remediation of soils contaminated with organic compounds: a review, Chem. Eng. J. 284 (2016) 582–598.
[3] G. Zeng, M. Chen, Z. Zeng, Risks of neonicotinoid pesticides, Science 340 (2013) 1403.
[4] G. Zeng, M. Chen, Z. Zeng, Shale gas: surface water also at risk, Nature 499 (2013) 154.
[5] D. Guaya, C. Valderrama, A. Farran, C. Armijos, J.L. Cortina, Simultaneous phosphate and ammonium removal from aqueous solution by a hydrated aluminum oxide modified natural zeolite, Chem. Eng. J. 271 (2015) 204–213.
[6] Z. Li, X. Tang, Y. Chen, Y. Wang, Behaviour and mechanism of enhanced phosphate sorption on loess modified with metals: equilibrium study, J. Chem. Technol. Biot. 84 (2009) 595–603.
[7] J.L. Gong, B. Wang, G.M. Zeng, C.P. Yang, C.G. Niu, Q.Y. Niu, W.J. Zhou, L. Yi, Removal of cationic dyes from aqueous solution using magnetic multi-wall carbon nanotube nanocomposite as adsorbent, J. Hazard. Mater. 164 (2009) 1517–1522.
[8] P. Xu, G.M. Zeng, D.L. Huang, C.L. Feng, S. Hu, M.H. Zhao, C. Lai, Z. Wei, C. Huang, G.X. Xie, Use of iron oxide nanomaterials in wastewater treatment: a review, Sci. Total. Environ. 424 (2012) 1–10.

[9] F. Yuan, J.L. Gong, G.M. Zeng, Q.Y. Niu, H.Y. Zhang, C.G. Niu, J.H. Deng, M. Yan, Adsorption of Cd (II) and Zn (II) from aqueous solutions using magnetic hydroxyapatite nanoparticles as adsorbents, Chem. Eng. J. 162 (2010) 487–494.

[10] X.J. Hu, J.S. Wang, Y.G. Liu, X. Li, G.M. Zeng, Z.L. Bao, X.X. Zeng, A.W. Chen, F. Long, Adsorption of chromium (VI) by ethylenediamine-modified cross-linked magnetic chitosan resin: isotherms, kinetics and thermodynamics, J. Hazard. Mater. 185 (2011) 306–314.

[11] K. Usharani, P. Lakshmanaperumalsamy, M. Muthukumar, Biological removal of phosphate from synthetic wastewater using bacterial consortium, Iran, J. Biotechnol. 9 (2011) 37–49.

[12] T. Fan, Y. Liu, B. Feng, G. Zeng, C. Yang, M. Zhou, H. Zhou, Z. Tan, X. Wang, Biosorption of cadmium(II), zinc(II) and lead(II) by *Penicillium simplicissimum*: isotherms, kinetics and thermodynamics, J. Hazard. Mater. 160 (2008) 655–661.

[13] L. Tang, G.M. Zeng, G.L. Shen, Y.P. Li, Y. Zhang, D.L. Huang, Rapid detection of picloram in agricultural field samples using a disposable immunomembrane-based electrochemical sensor, Environ. Sci. Technol. 42 (2008) 1207–1212.

[14] J.P. Chen, M.L. Chua, B. Zhang, Effects of competitive ions, humic acid, and pH on removal of ammonium and phosphorous from the synthetic industrial effluent by ion exchange resins, Waste. Manage. 22 (2002) 711–719.

[15] F. Long, J.L. Gong, G.M. Zeng, L. Chen, X.Y. Wang, J.H. Deng, Q.Y. Niu, H.Y. Zhang, X.R. Zhang, Removal of phosphate from aqueous solution by magnetic Fe–Zr binary oxide, Chem. Eng. J. 171 (2011) 448–455.

[16] C. Zhang, C. Lai, G. Zeng, D. Huang, C. Yang, Y. Wang, Y. Zhou, M. Cheng, Efficacy of carbonaceous nanocomposites for sorbing ionizable antibiotic sulfamethazine from aqueous solution, Water. Res. 95 (2016) 103–112.

[17] H.P. Wu, C. Lai, G.M. Zeng, J. Liang, J. Chen, J.J. Xu, J. Dai, X.D. Li, J.F. Liu, M. Chen, L.H. Lu, L. Hu, J. Wan, The interactions of composting and biochar and their implications for soil amendment and pollution remediation: a review, Crit. Rev. Biotechnol. (2016) 1–11.

[18] P. Song, Z. Yang, H. Xu, J. Huang, X. Yang, L. Wang, Investigation of influencing factors and mechanism of antimony and arsenic removal by electrocoagulation using Fe-Al electrodes, Ind. Eng. Chem. Res. 53 (2014) 12911–12919.

[19] S.G. Lu, S.Q. Bai, L. Zhu, H.D. Shan, Removal mechanism of phosphate from aqueous solution by fly ash, J. Hazard. Mater. 161 (2009) 95–101.

[20] S. Tanada, M. Kabayama, N. Kawasaki, T. Sakiyama, T. Nakamura, M. Araki, T. Tamura, Removal of phosphate by aluminum oxide hydroxide, J. Colloid Interface Sci. 257 (2003) 135–140.

[21] T.J. Daou, S. Begin-Colin, J.M. Grenèche, F. Thomas, A. Derory, P. Bernhardt, P. Legaré, G. Pourroy, Phosphate adsorption properties of magnetite-based nanoparticles phosphate adsorption properties of magnetite-based nanoparticles, Chem. Mater. 19 (2007) 4494–4505.

[22] H. Wu, D. Jiang, P. Cai, X. Rong, Q. Huang, Effects of low-molecular-weight organic ligands and phosphate on adsorption of *Pseudomonas putida* by clay minerals and iron oxide, Colloid Surface B 82 (2011) 147–151.

[23] Y. Zhou, L. Tang, G. Yang, G. Zeng, Y. Deng, B. Huang, Y. Cai, J. Tang, J. Wang, Y. Wu, Phosphorus-doped ordered mesoporous carbons embedded with Pd/Fe bimetal nanoparticles for the dechlorination of 2,4-dichlorophenol, Catal. Sci. Technol. 6 (2015) 1930–1939.

[24] Y. Zhou, L. Tang, G. Zeng, C. Zhang, Y. Zhang, X. Xie, Current progress in biosensors for heavy metal ions based on DNAzymes/DNA molecules functionalized nanostructures: a review, Sensor. Actuat. B-Chem. 223 (2016) 280–294.

[25] S. Karaca, A. Gürses, M. Ejder, M. Açıkyıldız, Adsorptive removal of phosphate from aqueous solutions using raw and calcinated dolomite, J. Hazard. Mater. 128 (2006) 273–279.

[26] Z.L. Shi, F.M. Liu, S.H. Yao, Adsorptive removal of phosphate from aqueous solutions using activated carbon loaded with Fe(III) oxide, Carbon 26 (2011) 299–306.

[27] M.R. Awual, A. Jyo, T. Ihara, N. Seko, M. Tamada, K.T. Lim, Enhanced trace phosphate removal from water by zirconium(IV) loaded fibrous adsorbent, Water. Res. 45 (2011) 4592–4600.

[28] Y. Su, H. Cui, Q. Li, S. Gao, J.K. Shang, Strong adsorption of phosphate by amorphous zirconium oxide nanoparticles, Water. Res. 47 (2013) 5018–5026.

[29] X. Dou, Y. Zhang, H. Wang, T. Wang, Y. Wang, Performance of granular zirconium–iron oxide in the removal of fluoride from drinking water, Water. Res. 45 (2011) 3571–3578.

[30] J. Zheng, Q. Zhao, Z. Ye, Preparation and characterization of activated carbon fiber (ACF) from cotton woven waste, Appl. Surf. Sci. 299 (2014) 86–91.

[31] S. Yao, J. Li, Z. Shi, Immobilization of TiO_2 nanoparticles on activated carbon fiber and its photodegradation performance for organic pollutants, Particuology 08 (2010) 272–278.

[32] Z. Sun, Y. Yu, S. Pang, D. Du, Manganese-modified activated carbon fiber (Mn-ACF): novel efficient adsorbent for Arsenic, Appl. Surf. Sci. 284 (2013) 100–106.

[33] Q. Zhou, X. Wang, J. Liu, L. Zhang, Phosphorus removal from wastewater using nano-particulates of hydrated ferric oxide doped activated carbon fiber prepared by Sol-Gel method, Chem. Eng. J. 200–202 (2012) 619–626.

[34] L. Zhang, M. Li, Y. Gao, J.Y. Liu, Y.F. Xu, Performance and mechanism study on phosphate adsorption onto activated carbon fiber loading lanthanum and iron oxides, Desalin. Water. Treat. 57 (10) (2016) 4671–4680.

[35] A. Sarkar, S.K. Biswas, P. Pramanik, Design of a new nanostructure comprising mesoporous ZrO_2 shell and magnetite core (Fe_3O_4@mZrO_2) and study of its phosphate ion separation efficiency, J. Mater. Chem. 20 (2010) 4417–4424.

[36] G. Mckay, A. Mesdaghinia, S. Nasseri, M. Hadi, M.S. Aminabad, Optimum isotherms of dyes sorption by activated carbon: fractional theoretical capacity & error analysis, Chem. Eng. J. 251 (2014) 236–247.

[37] A. Günay, E. Arslankaya, İ. Tosun, Lead removal from aqueous solution by natural and pretreated clinoptilolite: adsorption equilibrium and kinetics, J. Hazard. Mater. 146 (2007) 362–371.

[38] N.Y. Acelas, B.D. Martin, D. López, B. Jefferson, Selective removal of phosphate from wastewater using hydrated metal oxides dispersed within anionic exchange media, Chemosphere 119 (2015) 1353–1360.

[39] Y. Su, W. Yang, W. Sun, Q. Li, J.K. Shang, Synthesis of mesoporous cerium–zirconium binary oxide nanoadsorbents by a solvothermal process and their effective adsorption of phosphate from water, Chem. Eng. J. 268 (2015) 270–279.

[40] Y. Zhang, G.M. Zeng, L. Tang, D.L. Huang, X.Y. Jiang, Y.N. Chen, A hydroquinone biosensor using modified core–shell magnetic nanoparticles supported on carbon paste electrode, Biosens. Bioelectron. 22 (2007) 2121–2126.

[41] D.L. Huang, G.M. Zeng, C.L. Feng, S. Hu, X.Y. Jiang, L. Tang, F.F. Su, Y. Zhang, W. Zeng, H.L. Liu, Degradation of lead-contaminated lignocellulosic waste by *Phanerochaete chrysosporium* and the reduction of lead toxicity, Environ. Sci. Technol. 42 (2008) 4946–4951.

[42] L.A. Rodrigues, Adsorption kinetic, thermodynamic and desorption studies of phosphate onto hydrous niobium oxide prepared by reverse microemulsion method, Adsorption 16 (2010) 173–181.

[43] Y. Tang, E. Zong, H. Wan, Z. Xu, S. Zheng, D. Zhu, Zirconia functionalized SBA-15 as effective adsorbent for phosphate removal, Microporous Microporous Mater. 155 (2012) 192–200.

[44] H. Liu, X. Sun, C. Yin, C. Hu, Removal of phosphate by mesoporous ZrO_2, J. Hazard. Mater. 151 (2008) 616–622.

[45] Y.F. Lin, H.W. Chen, Y.C. Chen, C.S. Chiou, Application of magnetite modified with polyacrylamide to adsorb phosphate in aqueous solution, J. Taiwan Inst. Chem. E 44 (2013) 45–51.

[46] H. Jiang, P. Chen, S. Luo, X. Tu, Q. Cao, M. Shu, Synthesis of novel nanocomposite Fe_3O_4/ZrO_2/chitosan and its application for removal of nitrate and phosphate, Appl. Surf. Sci. 284 (2013) 942–949.

[47] M.H. Dehghani, M. Ghadermazi, A. Bhatnagar, P. Sadighara, G. Jahed-Khaniki, B. Heibati, G. Mckay, Adsorptive removal of endocrine disrupting bisphenol A from aqueous solution using chitosan, J. Environ. Chem. Eng. 4 (2016) 2647–2655.

[48] W. Song, B. Gao, X. Xu, F. Wang, N. Xue, S. Sun, W. Song, R. Jia, Adsorption of nitrate from aqueous solution by magnetic amine-crosslinked biopolymer based corn stalk and its chemical regeneration property, J. Hazard. Mater. 304 (2015) 280–290.

[49] H. Cui, Q. Li, S. Gao, J.K. Shang, Strong adsorption of arsenic species by amorphous zirconium oxide nanoparticles, J. Ind. Eng. Chem. 18 (2012) 1418–1427.

[50] C. Liang, Z. Xin, B. Pan, W. Zhang, H. Ming, L. Lu, W. Zhang, Preferable removal of phosphate from water using hydrous zirconium oxide-based nanocomposite of high stability, J. Hazard. Mater. 284 (2015) 35–42.

[51] J. Liu, Z. Qi, J. Chen, Z. Ling, C. Ning, Phosphate adsorption on hydroxyl–iron–lanthanum doped activated carbon fiber, Chem. Eng. J. 215–216 (2013) 859–867.

[52] E. Zong, D. Wei, H. Wan, S. Zheng, Z. Xu, D. Zhu, Adsorptive removal of phosphate ions from aqueous solution using zirconia-functionalized graphite oxide, Chem. Eng. J. 221 (2013) 193–203.